Lasers in Surgery and Medicine 18:278–293 (1996)

# Effect of Pulse Duration on Bubble Formation and Laser-Induced Pressure Waves During Holmium Laser Ablation

**E. Duco Jansen, PhD, Thomas Asshauer, MSc, Martin Frenz, PhD, Massoud Motamedi, PhD, Guy Delacrétaz, PhD, and Ashley J. Welch, PhD**

*Biomedical Engineering Program, University of Texas, Austin, 78712 (E.D.J., A.J.W.); Biomedical Laser and Spectroscopy Program, University of Texas Medical Branch, Galveston, 77555 (M.M.); Laboratory of Applied Optics, Swiss Federal Institute of Technology, CH-1015 Lausanne, Switzerland (T.A., G.D.); Institute of Applied Physics, University of Berne, CH-3112 Berne, Switzerland (M.F.)*

***Background and Objective:*** **One concern during laser ablation of tissue is the mechanical injury that may be induced in tissue in the vicinity of the ablation site. This injury is primarily due to rapid bubble expansion and collapse or due to laser-induced pressure waves. In this study, the effect of laser pulse duration on the thermodynamics of bubble formation and accompanying acoustic pressure wave generation has been investigated.**
***Study Design/Materials and Methods:*** **Q-switched holmium:YAG laser pulses (pulse duration 500 ns, pulse energy 14 mJ) and free-running holmium:YAG laser pulses (pulse duration 100–1,100 μs, pulse energy 200 mJ) were delivered in water and tissue phantoms via a 200- and 400-μm fiber, respectively. The tissue phantoms consisted of polyacrylamide gels with varying mechanical strengths. Bubble formation was recorded with a fast flash photography setup, while acoustic transients were measured with a needle hydrophone.**
***Results:*** **It was observed that, as the pulse length was increased the bubble shape changed from almost spherical for Q-switched pulses to a more elongated cylinder shape for longer pulse durations. The bubble expansion velocity was larger for shorter pulse durations. Only the Q-switched pulse induced a measurable thermo-elastic expansion wave. All pulses that induced bubble formation generated pressure waves upon collapse of the bubble in gels as well as in water. However, the magnitude of the pressure wave depended strongly on the size and geometry of the induced bubble.**
***Conclusion:*** **The magnitude of the collapse pressure wave decreased as laser pulse duration increased. Hence it may be possible to reduce collateral mechanical tissue damage by stretching the holmium laser pulse.** 

Key words: acoustics, bubble, cavitation, infrared laser, pulse length, tissue phantoms

## INTRODUCTION

In many medical applications where high power laser energy is delivered via an optical fiber, the goal is removal of tissue with minimal damage to surrounding tissue. Pulsed lasers are

Accepted for publication March 20, 1995.

Address reprint requests to E. Duco Jansen, Biomedical Engineering Program, ENS 614A, University of Texas, Austin TX 78712.

typically chosen over continuous wave devices to minimize thermal damage and provide precise control of the ablation process [1]. Currently, the holmium:YAG laser at 2.12 μm is used experimentally in a variety of medical specialties for the precise removal of tissue since its wavelength is near the 1.94 μm absorption peak of water. The 2.12 μm energy can be transmitted through low OH fibers, which makes this wavelength particularly attractive for minimally invasive procedures.

At room temperature the penetration depth of 2.12 μm radiation in water is ~300 μm. Nevertheless, concerns have been raised about the extent of damage that may be produced by free-running (pulse duration ~ 250 μs) as well as Q-switched (pulse duration < 1 μs) Ho:YAG pulses. Dissections in vascular tissue during holmium laser angioplasty have been reported [2]. Van Leeuwen et al. [3] suggest that these dissections are produced by the expanding and collapsing phase of a bubble formed within tissue during the laser pulse. Laser-induced shock waves have been suggested as the cause of damage to endothelial cells when the surface of the cornea is irradiated with Q-switched erbium laser pulses [4]. For the currently used high pulse energies in orthopedic applications, there is an additional concern of destruction of the fiber delivery system due to laser-induced pressure waves.

## Pressure Transients

In absorbing samples, two mechanisms of stress wave generation are encountered that dominate stress generation at modest irradiance levels where dielectric breakdown is absent; these are thermo-elastic effect and ablative recoil stress. The generation of stress waves by the thermo-elastic effect in liquids and solids by pulsed lasers has been studied extensively since the early days of laser [5,6]. Most materials expand upon heating as an increase in temperature leads, on average, to a larger equilibrium atomic spacing. The expansion is driven by internal forces and if this is hindered, large stresses develop. This occurs in the case of a constrained body or material inertia under conditions of rapid heating, when the conditions of stress confinement are met. This is known as the thermo-elastic effect. In this case, the laser pulse duration is shorter than the time it takes for the pressure transient to cross the penetration depth of the laser light [7,8]:

$$\tau_p < \frac{\delta}{\sigma} \quad (1)$$

where $\tau_p$ is the laser pulse duration (s), $\delta$ is the penetration depth (mm), and $\sigma$ is the sound velocity (mm/s). These acoustic transients, which may have an amplitude of 1 kbar or more, are dependent on the material properties (especially the absorption coefficient), sound velocity in the medium, laser pulse duration, and pulse energy [9,10]. As a sound wave travels through a material, the local pressure increases and decreases, thus leading to transient variations in density and temperature of the material.

## Bubble Formation

It has been show by van Leeuwen et al. [11] and others that at radiant exposures associated with tissue ablation (~930 J/cm$^2$), a steam bubble starts to form at the tip (320 μm) of the fiber ~10–20 μs after the onset of the laser pulse, and the bubble grows to a maximum volume in ~200–300 μs and then collapses [11]. The time of onset of bubble formation and the maximum radius of the bubble are a function of the energy and the pulse duration of the laser pulse. Once sufficient energy is deposited to initiate vaporization, further radiation passes through the expanding bubble and is absorbed at the distal surface of the bubble. Long pulse radiation (250 μs) causes continued vaporization after the initiation of the bubble, producing a pear-shaped bubble [11,12]. In contrast, Q-switched (<1 μs) radiation creates a spherical bubble since all light energy is delivered to the water before a bubble is formed [13].

Several groups have found that rather large shock waves can be produced in water with long pulse (free-running) Ho:YAG laser radiation delivered by a fiber inserted into the water, although there is no stress confinement under these irradiation conditions [12,14]. These classic cavitation-induced shock waves are produced as energy associated with the bubble is converted to acoustic energy upon collapse of the bubble [15]. It has been known for more than a century that upon collapse of these cavities, regardless of their source, an acoustic transient is generated. Although much of the research has been related to under water explosions, many of the findings and concepts also hold for the underwater delivery of highly absorbed pulsed laser energy [16].

Because of the distorted shape of the bubbles formed by long laser pulses, segments of the bub-

ble may collapse at slightly different times producing multiple, smaller shock waves [12,17]. An excellent overview of the theory and experimental descriptions of laser-induced shock waves in water can be found in [8,18].

It should be mentioned that the process of under-water ablation is inherently different from ablation at an air-water interface. In the latter case, a positive pressure wave will be reflected on the free surface and turn into a symmetric bipolar wave. Much work has been done describing the effect of these tensile waves on tissues and fluid surfaces, causing cavitation bubbles and processes such as spallation [19,20].

Since there is an increasing concern about the effect of acoustic transients on biological tissues and optical fibers during medical applications, this study has been designed to measure the acoustic pressures associated with the holmium laser ablation of tissue phantoms. The objective of this study was to investigate the effect of the pulse duration of a holmium:YAG laser on bubble formation and acoustic pressure transient generation in water and tissue phantoms. We have investigated a large range of pulse durations (500 ns–1.1 ms). By using a fast flash photography setup and a PVDF needle hydrophone, we can relate the process of bubble formation to the generation of acoustic transients. In addition, tissue phantoms mechanical strengths were characterized by their Young's modulus and the effect of tissue strength on bubble formation and pressure wave generation was examined.

## MATERIALS AND METHODS

### Experimental Setup

A Schwartz Electro Optics 1-2-3 laser was used to generate Ho:YAG ($\lambda$ = 2.12 $\mu$m) laser light. The laser had a variable pulse width power supply that allowed us to change the pulse duration of the laser in the free-running mode. Laser pulses with a pulse energy of 200 ± 5 mJ and pulse durations of 260 $\mu$s (210 $\mu$s FWHM), 460 $\mu$s (400 $\mu$s FWHM), and 1,100 $\mu$s (1,050 $\mu$s FWHM) were generated in the free-running mode. The laser was equipped with an acousto-optical Q-switch, which provided laser pulses with a pulse energy of 14 ± 1 mJ and a pulse duration of 500 ns. In addition, free-running mode pulses with a pulse energy of 200 mJ and a duration of 100 $\mu$s were generated by using the Q-switch as a pulse gate. Laser light in the free-running mode was coupled into a 400 $\mu$m low OH fiber and laser light in the Q-switched mode was coupled into a 200 $\mu$m diameter low OH fiber. The resulting radiant exposures were 1,592 mJ/mm$^2$ and 446 mJ/mm$^2$, respectively. The laser pulse repetition rate was always 2 Hz.

The last centimeter of the cladding at the distal end of the fiber was removed and the fiber was positioned in a transparent container filled with deionized water at room temperature. The processes taking place at the fiber end were monitored using a standard fast flash photography setup as described elsewhere [11]. The illumination source used was a nitrogen pumped dye laser ($\lambda$ = 580 nm) with a pulse duration of 900 ps (P.R.A. International). This laser was synchronized with the Ho:YAG laser via a delay generator (Stanford Research Systems DGD 535) so flash photographs were taken at variable delay times of 0–1,200 $\mu$s after the start of Ho:YAG laser pulse.

The acoustic measurements were made using a piezoelectric polyvinlyidenefluoride (PVDF) needle hydrophone (Imotec, Germany). The diameter of the active surface of the hydrophone was 0.5 mm and the rise time was 40 ns. The hydrophone was factory calibrated in water to give absolute pressure amplitudes. However, the absolute pressures may be underestimated due to the fact that the pressure pulses have been reported to have pulse widths of 10–30 ns [18]. A detector with a 40 ns response time will thus underestimate the absolute pressure values. The signal from the hydrophone was displayed on a 500 MHz digital storage oscilloscope (Tektronix). The hydrophone was placed in the container with water at a distance of ~2 mm from the fiber end. This distance ensured that the hydrophone was well out of the range of the expanding vapor bubble. For any parameter combination, a minimum of 10 pressure traces were recorded. The data are presented as the average ± standard deviation. Images recorded by the CCD camera that was used for the fast flash photography also provided an absolute measurement of the distance between the fiber end and the hydrophone tip. Pressure at any distance, $r$ from the center of the bubble was estimated assuming the amplitude of a spherical acoustic wave was inversely proportional to the distance, $r$ from the center [21–23].

### Media

**Polyacrylamide gels and water.** Fast flash photography of bubble formation and pressure wave measurements were made in water and

in tissue phantoms at room temperature. These tissue phantoms were a more realistic model for biological tissue than water, especially with regard to mechanical properties. In order to visualize the process of bubble formation, the phantom medium had to be transparent. Gels of polyacrylamide (PAA) were made with various water concentrations to simulate different tissue strengths. The gels that were used had polyacrylamide concentrations of 5%, 10%, 16%, 20%, or 25% (thus the water concentrations were 95%, 90%, 84%, 80%, or 75%). The gels were cut to blocks with dimensions of ~2 × 2 × 5 cm. A gel block was pinned to a holder and placed in the container, filled with deionized water. In the gel experiments, the fiber and the hydrophone were each mounted to a micrometer and slowly positioned in the gel under guidance of the CCD imaging system. Once the fiber and hydrophone were positioned inside the gel block, the laser was activated, and only one pulse of holmium laser energy was delivered to the gel by opening a shutter in the laser beam. The bubble formed inside the gel was recorded at its maximum size. The time for maximum size was determined by giving a few initial pulses and measuring the time to collapse from the hydrophone signal. Knowing that the maximum bubble size occurs just past the half life time of the bubble, the delay was set to this time. To obtain reproducible results, only the bubble induced by the first laser pulse was recorded. Once the gel was disrupted by the first bubble, the behavior due to subsequent bubbles was affected. A fresh piece of gel was used for every pulse.

In water, the entire bubble formation sequence was recorded. The traces from the acoustic transducer during the laser pulse delivery and subsequent bubble formation, collapse and (multiple) rebounds were recorded on the oscilloscope and stored for analysis.

Mechanical properties of phantom media as a function of water concentration of the gels were quantified by determining the stress-strain relation of all the gels and calculating the elasticity modulus (or Young's modulus). A slab of gel was cut to a thickness, L, of 10–15 mm. The slab of gel was placed on a digital balance and a metal rod with a diameter of 3.15 mm was placed above the gel. The metal rod was mounted to a micrometer and the rod was translated into the gel. The force was read from the digital balance after every 100 μm of translation up to the equivalent of 95 g (the maximum range of the balance) or 3.5 mm, whichever came first. A plot was made of the stress = force/area ($N/m^2$) against the dimensionless strain = $\Delta L/L$. The slope of this linear curve represented the Young's modulus of the material ($N/m^2$).

**TABLE 1. Values of Measured Young's Moduli for Various Concentrations of Polyacrylamide Gels***

| Material | Young's modulus ($10^6$ $N/m^2$) | r |
|---|---|---|
| PAA gel 95% water | 0.031 | 0.99 |
| PAA gel 90% water | 0.173 | 0.99 |
| PAA gel 84% water | 0.464 | 0.99 |
| PAA gel 80% water | 0.651 | 0.99 |
| PAA gel 75% water | 0.866 | 0.99 |
| Thoracic aorta | 0.3–0.94 | ——— |
| Abdominal aorta | 0.98–1.42 | ——— |
| Meniscus | 0.41 | ——— |

*Also shown are values of Young's modulus for some biological tissues that were obtained from the literature [24]. Note that the range of Young's moduli covered by the polyacrylamide gels is on the same order of magnitude as the tissues.

Although Young's modulus is not defined for liquids, the measurements of bubble size and pressure waves made in water were plotted with the gel data against the Young's modulus. For this purpose the value for the Young's modulus in water was arbitrarily set to be zero.

**Tissue.** A series of in vitro experiments in tissue were performed with the Q-switched laser. The abdominal aorta and the meniscus of a dog were excised within 30 minutes after death. Tissue samples were harvested and stored in saline moist cloth at 4°C until the moment of use. The samples were used within 6 hours after death. The delivery fiber and the hydrophone were placed in contact (with minimal force, <1 g) on the tissue. In the tissue experiments, only the acoustic measurements were made.

## RESULTS

The values for the Young's modulus of the gels at different concentrations are presented in Table 1. Values for the Young's modulus were obtained by fitting the stress-strain curve to a linear curve using a least-squares fit. In the same table elasticity moduli of several tissues, obtained from the literature, are shown [24].

### Bubble Dimensions in Water

A compilation of the bubble expansion and collapse sequence in water at room temperature for laser pulse durations of 500 ns, 100 μs, 260 μs, 460 μs, and 1,100 μs is presented in Figure 1. In

general, the bubble is more pear shaped for longer pulse durations whereas the bubble is almost spherical for short pulse durations. The expansion phase of the bubble is fairly reproducible and constant from pulse to pulse, whereas the collapse phase, especially for the longer pulse durations, is chaotic. Upon collapse of the bubble, in particular those formed by short laser pulse durations, the bubble reexpands and collapses again. In water, up to four cycles of collapse and reexpansion have been observed for the Q-switched pulse induced bubble. However, it is expected that only the initial expansion and collapse cycle are important for tissue effects.

In the longer pulse-induced bubble, a quasi steady state is reached; parts of the bubble close to the fiber that were formed first collapse, while other parts of the bubble, farther away from the fiber, are still expanding. The result is some sort of oscillation of the bubble, which appears on the pictures as an "hour-glass" shaped bubble. In contrast to the bubbles induced by the short pulses (Q-switched, 100 μs and 260 μs), which show a real collapse phase and reexpansion of the bubble, the bubbles induced by the longer pulses (460 μs and 1,100 μs) do not collapse forcefully and do not reexpand. Instead, these bubbles just vanish (fade away) when no more laser energy is deposited into the bubble.

From the time-resolved photographs, bubble dimensions (width and length) have been measured and the results are shown in Figure 2a,b. Every data point is the average (± standard deviation) of four measurements. It can be seen that the shorter pulse durations result in a faster bubble expansions as well as a faster bubble collapse. It should be noted that all the pulse energies for the different pulse durations are the same (200 ± 5 mJ), except for the Q-switched case, where the pulse energy is only 14 ± 1 mJ.

### Bubbles in Gels

The maximum size of a bubble in 84% gel (16% PAA) is presented in Figure 1 (far right column) for each pulse duration used in this experiment. In Figure 3 the maximum bubble dimensions are plotted against the elasticity moduli of the various gels for the Q-switched pulse and the 100 μs pulse duration. Every data point represents the average (± standard deviation) of five measurements. For stronger gels (i.e., higher values of the elasticity modulus), the bubble size, length as well as width, is smaller. It is, however, remarkable that for the 100 μs pulse duration in 90% and 95% gel concentrations, the bubble dimensions are larger than the bubble dimensions in water. This is not the case during the Q-switched laser pulses.

### Acoustic Transients: Expansion Wave

For the Q-switched laser pulse, which had a duration of ~500 ns and was the only pulse duration that came close to a situation of stress confinement, a pressure wave was measured that coincided in time with the laser pulse, delayed only by the time needed for the pressure wave to traverse the distance between the fiber and the hydrophone, given a speed of sound in water of 1,500 m/s. This thermo-elastic expansion wave occurred before bubble formation takes place. Figure 4a shows the trace of the hydrophone signal when a Q-switched laser pulse was delivered in water. The pressure waves that occurred at later times were generated due to the collapse of the vapor bubble. The initial pressure peak was not seen during any of the longer pulse durations (≥ 100 μs) (see Fig. 4b). In addition, the amplitude of this pressure wave did not change significantly as a function of the Young's modulus of the irradiated material as shown in Figure 5. For the Q-switched pulse with a pulse duration of 500 ns and a radiant energy of 14 mJ (radiant exposure = 445 mJ/mm$^2$) in water, the amplitude of this pressure wave at a distance of 1 mm from the fiber, was 40 ± 8 bars. Similar values were measured in all gel concentrations as well as in the tissues.

### Acoustic Transients: Collapse Wave

For radiant exposures above the threshold for ablation, bubble formation occurs, in water as well as in the polyacrylamide gels and most of the tissues. Upon collapse of these vapor cavities, an acoustic pressure wave is generated (see Fig. 4). The origin of the collapse wave coincides with the moment of collapse of the bubble. In some cases (if one is lucky enough to capture it), the pressure wave can be seen even with the fast flash photography setup, provided that a very short flash light is used (see Fig. 1). The pressure wave induces a discontinuity in density (i.e., in the index of refraction), which is visible in the picture as a dark ring around the collapse center that travels outward. In case of multiple bubble expansion and collapse cycles, multiple collapse waves are seen. The bubble collapse and the pressure wave that is generated due to the collapse are affected by a number of factors. The most import factors influ-

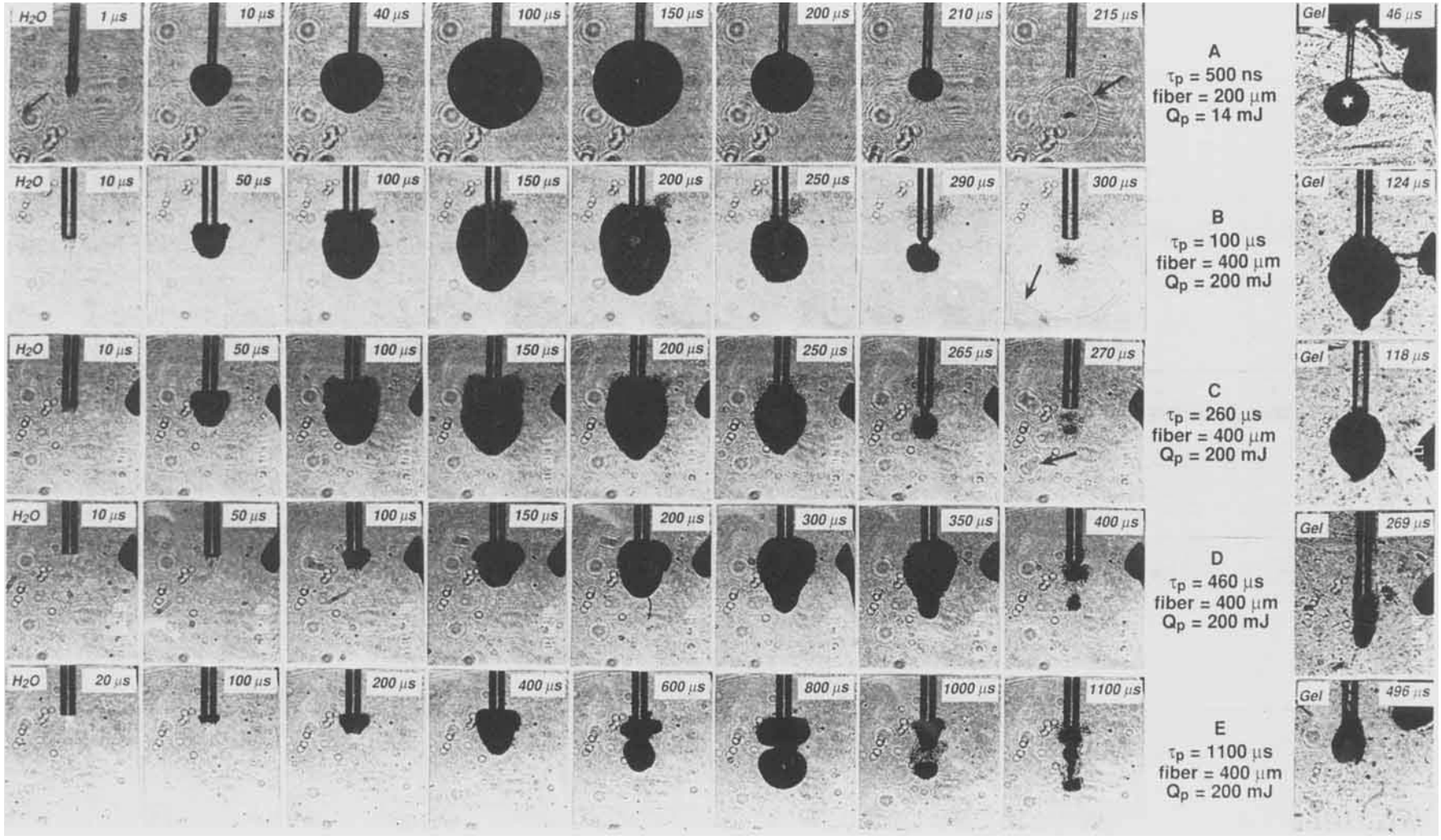


Fig. 1. Compilation of bubble expansion and collapse in water at room temperature for different laser pulse durations (500 ns, 100 μs, 260 μs, 460 μs, 1,100 μs), recorded using the fast flash photography setup with a nitrogen-pumped dye laser as flash light ($\tau_p$ <1 ns). The far right column shows the maximum bubble size in 84% water concentration polyacrylamide gel. Note that the fiber diameter for the 500 ns pulse was 200 μm and the pulse energy was 14 ± 1 mJ, whereas for all other pulse durations the fiber diameter was 400 μm and the pulse energy was 200 mJ. It can be seen that the bubble in the 84% water concentration gel is always smaller than in water for otherwise similar conditions. In addition, the gel has a tendency to distort the bubble geometry. (**A**) Pulse duration is 500 ns. Time elapsed since the start of the laser pulse is shown in the pictures. The arrow points at the expansion pressure wave in the 1 μs picture and the collapse pressure wave in the 215 μs picture. (**B**) Pulse duration is 100 μs. The arrow points at the collapse pressure wave in the 300 μs picture. (**C**) Pulse duration is 260 μs (210 μs FWHM). The arrow points at the collapse wave in the 270 μs picture. (**D**) Pulse duration is 460 μs (410 μs FWHM). (**E**) Pulse duration is 1,100 μs (1050 μs FWHM). Note the oscillating behavior of the bubble between 400 and 1,000 μs.

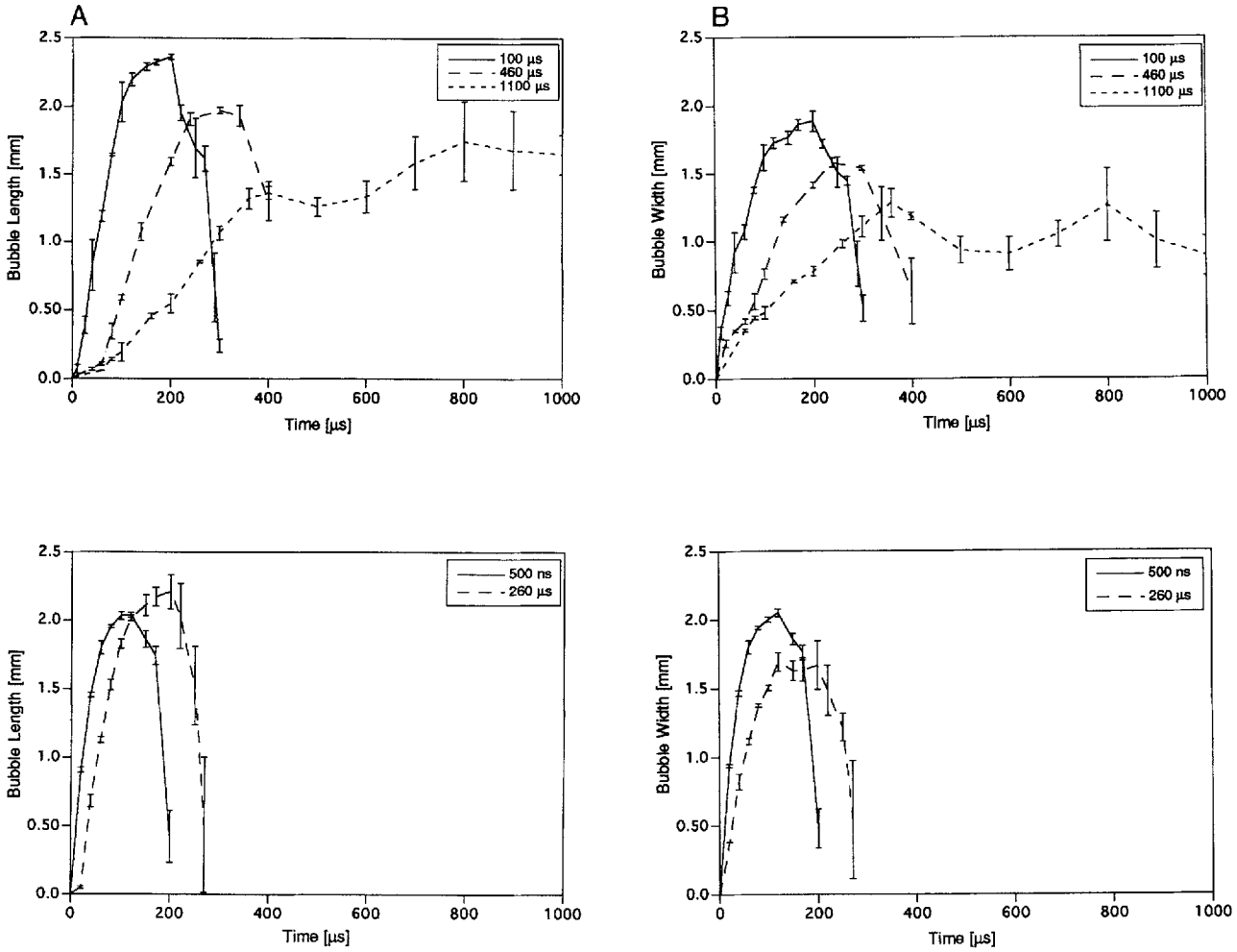


Fig. 2. Measured maximum bubble length (**A**) and width (**B**) as a function of time for different pulse durations (500 ns, 100 μs, 260 μs, 460 μs, and 1,100 μs). Plotted data points are the average of four measurements. Error bars represent the standard deviations.

encing the behavior of the collapse pressure wave are the bubble size and the bubble geometry. Since these parameters are strongly influenced by the pulse duration, the results for the different pulse durations are presented separately.

**Q-switched laser pulse.** The moment of collapse (i.e., the lifetime of the bubble) is directly related to the bubble size as shown in Figure 6. Also shown in Figure 6 is the theoretically expected relation between bubble diameter and bubble lifetime according to Lord Raleigh [15] and Cole [16]. The collapse wave occurs earlier in gels with lower water concentration (higher elasticity modulus) since the bubble size is smaller in these gels (Fig. 7a). The amplitude of the collapse wave is related to the bubble size (and thus bubble lifetime) as well (Fig. 7b). However, the amplitude of the collapse wave is highly variable, as indicated by the large standard deviations, possibly due to small geometrical differences in the bubble shape.

In aorta, where van Leeuwen et al. [3] reported a subsurface bubble, a collapse wave was also measured. In contrast, in meniscus, which is primarily cartilage tissue, no collapse wave was measured when the fiber was in good contact with the tissue. When only a slight amount of water was allowed between the fiber and the tissue, a bubble was formed (by vaporizing that water), which collapsed and generated a pressure wave.

**100 μs laser pulse.** The 100 μs long holmium pulse produces bubbles that are slightly elongated in water as well as in gels as seen in Figure 1. As a consequence, the collapse wave amplitudes are smaller than those observed during the collapse of the Q-switched laser pulse and typically consist of more than one peak due to the

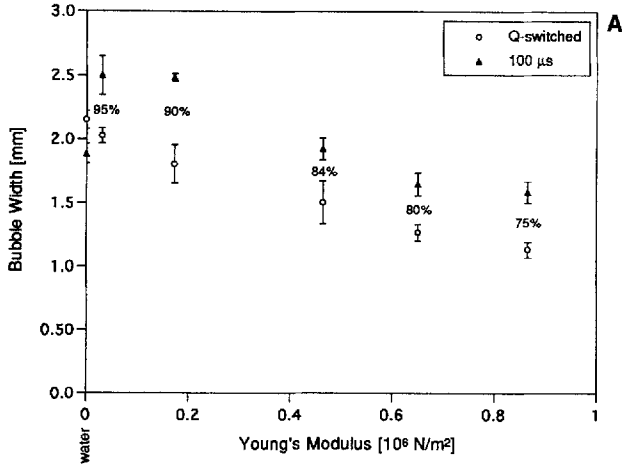


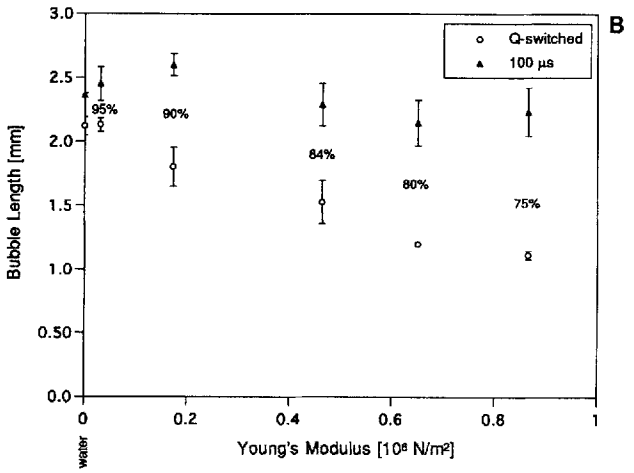


Fig. 3. Measured maximum bubble width (**A**) and length (**B**) as a function of the elasticity modulus of the gels for Q-switched pulse (500 ns, 14 mJ, 200 μm fiber) (○), and 100 μs pulse duration (200 mJ, 400 μm fiber) (▲). The data points are the average of four measurements and the error bars represent the standard deviation.

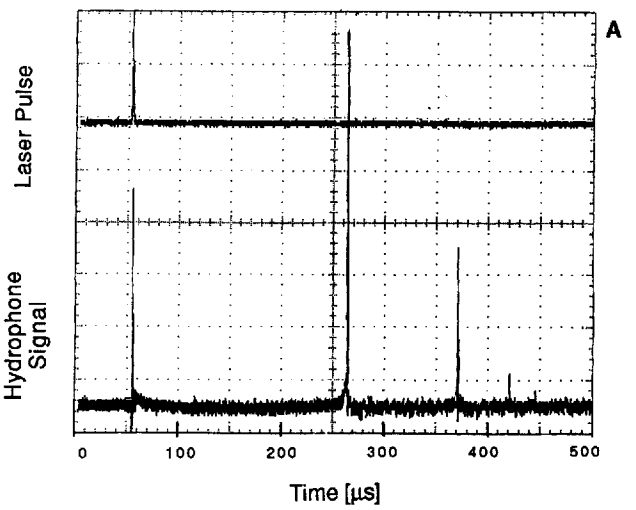


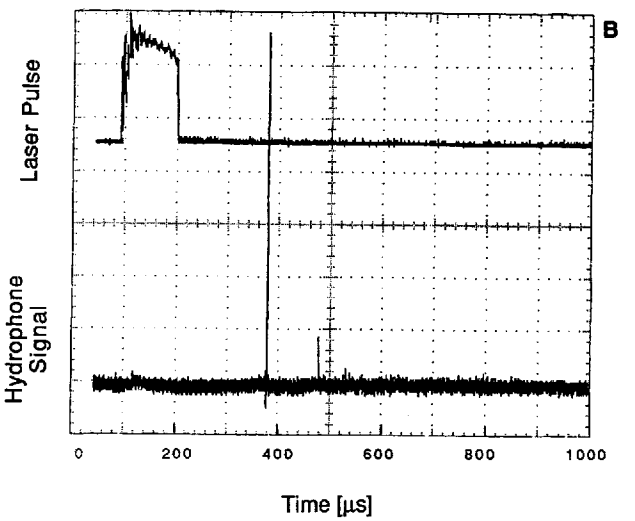


Fig. 4. Oscilloscope trace of the laser pulse measured with photo diode (top) and the pressure signal measured with the hydrophone (bottom). (**A**) Q-switched laser pulse, 500 ns, 14 ± 1 mJ, 200 μm fiber delivered in water at room temperature. Notice the expansion pressure wave that coincides with the laser pulse. Up to 4 collapse pressure waves can be seen in this trace. The horizontal scale is 50 μs/div. (**B**) 100 μs pulse duration, 200 ± 5 mJ, 400 μm fiber delivered in water at room temperature. Notice the lack of the expansion peak. Only two collapse pressure peaks can be seen. The horizontal scale is 100 μs/div.

fact that the elongated symmetry causes the bubble to collapse with more than one collapse center and not all at exactly the same time. The hydrophone trace during a 100 μs pulse in water is shown in Figure 4b. Note the absence of the initial expansion wave. Bubble lifetime and the collapse wave amplitude at a distance of 1 mm from the fiber tip as a function of the elasticity modulus of the gel are presented in a and b, respectively, of Figure 8. Again, the bubble lifetime and amplitude of the collapse wave are correlated (see also Fig. 6). It is remarkable that in the 95% and 90% water concentration gels, the bubble lifetime as well as the collapse amplitude are not smaller, but are slightly larger than in water. However, these results agree with the fact that the photographed bubbles in these gels were also slightly larger. For the gels with lower water concentrations (84%, 80%, and 75%), the bubble lifetime is shorter and the collapse amplitude is smaller than in low water concentration gels, but no significant differences can be seen between bubble lifetimes and collapse amplitudes induced in the 84%, 80%, and 75% gels.

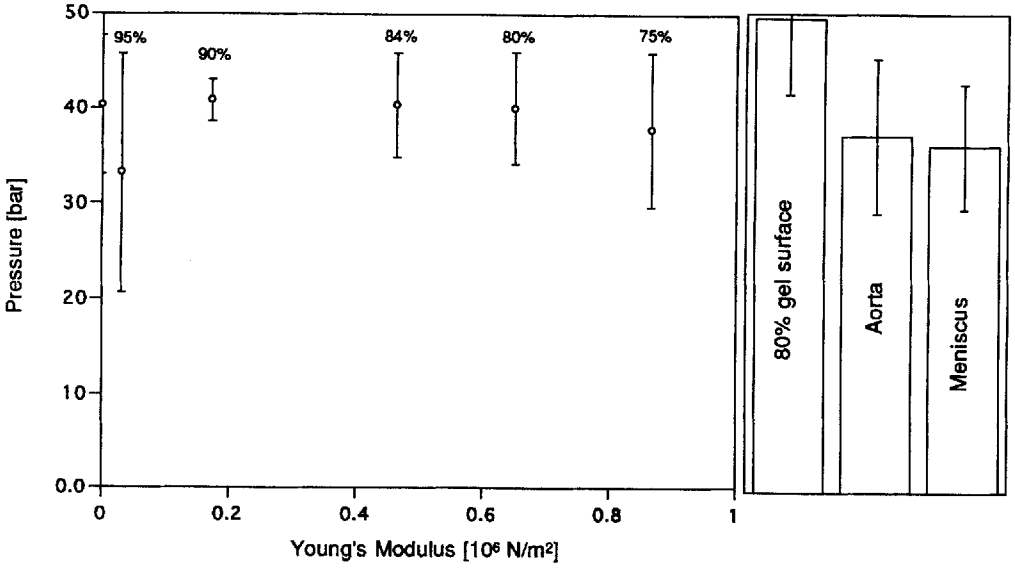


Fig. 5. Amplitude of the expansion pressure wave at a distance of 1 mm from the fiber, induced by the Q-switched laser (500 ns, 200 μm fiber, 14 ± 1 mJ) inside the gels plotted as a function of the elasticity modulus of the gels. On the right the expansion pressure amplitude measured at the surface of an 80% gel, canine aorta, and canine meniscus are plotted.

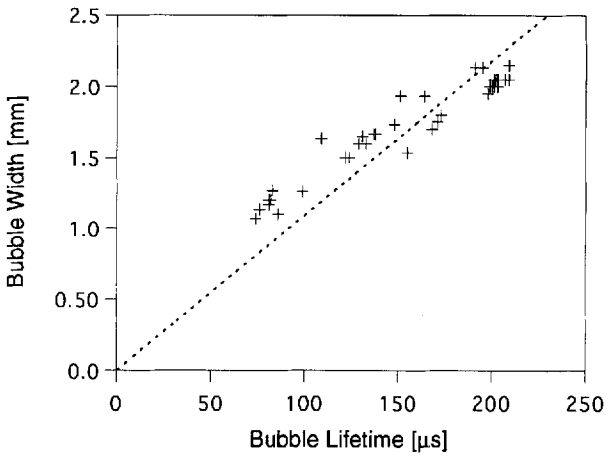


Fig. 6. Maximum bubble width as a function of the bubble lifetime. Bubbles were induced by a Q-switched holmium: YAG laser (500 ns, 200 μm fiber, 14 ± 1 mJ) in water and all gel concentrations. It can be seen that the bubble lifetime and size are correlated regardless of the material properties of the material in which the bubble was produced. Also plotted is the theoretically predicted relation between bubble diameter and bubble lifetime [15,16]

**Longer pulse durations.** Pulse duration was varied to determine if there was a value that minimized the pressure wave associated with bubble collapse. Laser pulses with a pulse energy of 200 mJ and pulse durations of 260 μs (210 μs FWHM), 460 μs (400 μs FWHM), and 1,100 μs (1050 μs FWHM) were delivered in water and 84% (16% PAA) polyacrylamide gel, a concentration that was representative of soft tissue.

The collapse pressure wave amplitudes and bubble lifetimes due to these longer pulses are shown in a and b, respectively, of Figure 9. The 100 μs and the 260 μs laser pulse caused rapid bubble collapse and an associated pressure wave. For pulse durations of 460 μs (410 μs FWHM) and above, the amplitude of the collapse pressure waves in water was less than nine bars at a distance of 1 mm from the end of the delivery fiber, as compared to 66 and 54 bars for the 100 μs and 260 μs pulse durations. Pressure transients were less than the noise level (2 bar) in 95% of the measurements of the acoustic transient owing to 1,100 μs pulse durations. Of the 1,100 μs laser pulses that did induce collapse pressure waves, the average collapse pressure in water was 7.5 bar.

In 84% water concentration gel, no pressure transients larger than the noise level (2 bar) were measured during the 460 μs laser pulse. The average bubble lifetime for the 460 μs pulse was 418 μs. For the 1,100 μs pulse duration, parts of the bubble collapsed at different times during the laser pulse. Consequently, characterization of bubble lifetime by the initial collapse was not possible. In gel, no pressure transients larger than the noise level were measured.

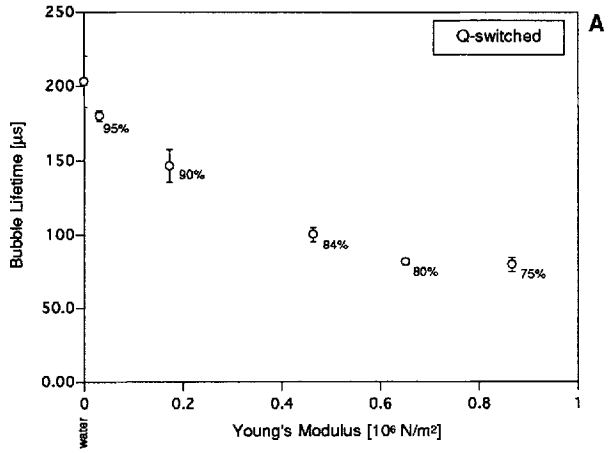


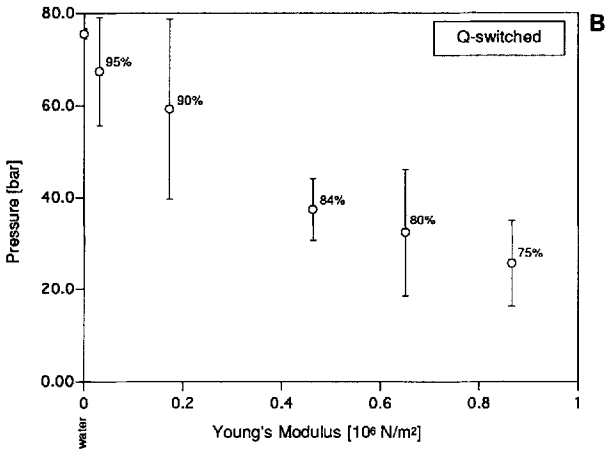


Fig. 7. (**A**) Bubble lifetime of Q-switched laser (500 ns, 14 mJ, 200 µm fiber) induced bubbles in water and gels plotted as a function of the elasticity modulus of the gel. It can be seen that the stronger gels limit the bubble lifetime due the fact that the bubbles are smaller. (**B**) Collapse pressure amplitude of Q-switched laser (500 ns, 14 mJ, 200 µm fiber) induced bubbles at a distance of 1 mm from the fiber tip, in water and gels plotted as a function of the elasticity modulus of the gel. Note that the collapse pressure is reduced for stronger gels due to the fact that the bubble size is limited by the mechanical strength of the gel.

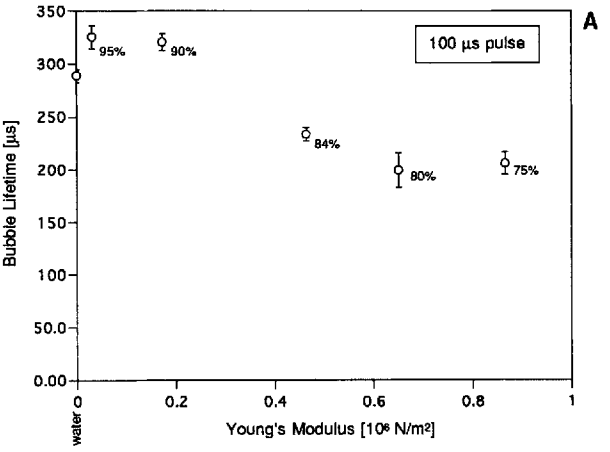


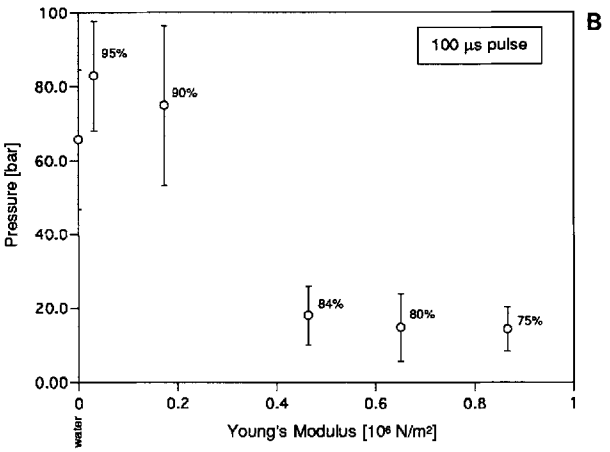


Fig. 8. (**A**) Bubble lifetime of laser-induced bubbles in water and gels induced by a 100 µs long holmium:YAG pulse with an energy of 200 ± 5 mJ (400 µm fiber), plotted as a function of the elasticity modulus of the gel. It can be seen that the stronger gels limit the bubble lifetime due the fact that the bubbles are smaller. Note that the effect is less significant as compared to the Q-switched pulse (Fig. 7A). (**B**) Collapse pressure amplitude at a distance of 1 mm from the fiber tip of laser-induced bubbles in water and gels induced by a 100 µs long holmium:YAG pulse with an energy of 200 ± 5 mJ (400 µm fiber), plotted as a function of the elasticity modulus of the gel. Note that the collapse pressure is reduced for stronger gels due to the fact that the bubble size is limited by the mechanical strength of the gel.

## DISCUSSION

The goal of this study was to investigate the effect of the pulse duration of a holmium:YAG laser pulse on the explosive bubble formation process and on the pressure transient generation during laser pulse delivery and bubble collapse in water and in tissue phantoms.

### Validity of the Tissue Model

Our first concern about the tissue phantoms is how good a model they are for biological tissue and what the limitations are. The gels are made with water concentrations that are comparable to biological soft tissues (> 75%). Hence, since the holmium wavelength is primarily absorbed by water [25,26], the gels are optically a reasonable model for soft tissue. Thermally, the density, $\rho$, the heat capacity, $c$, the thermal conductivity, $k$, of the gel reasonably can be assumed to be similar

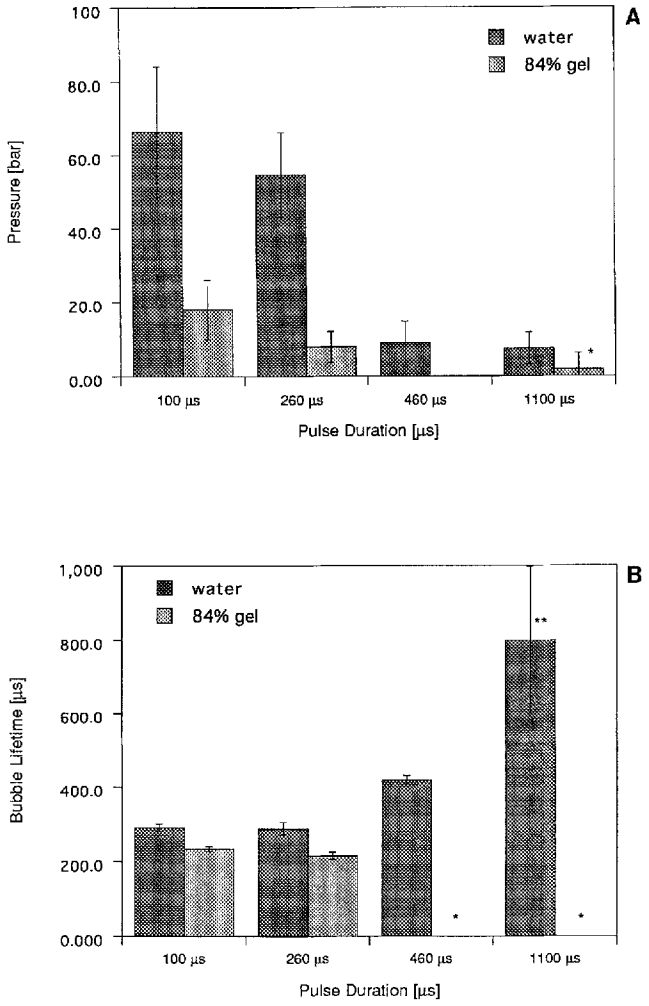


Fig. 9. (A) Collapse pressure at 1 mm from the fiber tip in water and 84% gel for different laser pulse durations (100 µs, 260 µs, 460 µs, and 1,100 µs). The collapse pressure is significantly reduced for longer pulse durations in water as well as in gel. Every data point is the average of at least five measurements. The error bars represent the standard deviations. [*] for the 1,100 µs pulse in gel, 95% of the pulses given showed no collapse pressure larger than the noise at all (~2 bar). (B) Collapse time in water and 84% gel for different laser pulse durations (100 µs, 260 µs, 460 µs, and 1,100 µs). Every data point is the average of at least five measurements. The error bars represent the standard deviations. Note that the collapse time is always smaller in gel compared to water. [*] For the 460 µs pulse in gel, no collapse pressure larger than the noise at all (~2 bar) was measured. Therefore the collapse signal cannot be used as a measurement for the bubble lifetime. [**] For the 1,100 µs pulse in water, parts of the bubble collapse during the pulse delivery and produce small pressure transients. Therefore the collapse signal cannot be used as a measurement for the bubble lifetime.

to water. The thermal properties of water are often used to represent soft tissue. In addition, like tissue, the polyacrylamide gels do not melt at elevated temperatures, unlike other gels such as gelatin or agar.

Most important for the process of bubble formation are the mechanical properties. The process of bubble formation is a highly dynamic process. Typically, mechanical properties of materials that are measured and reported in the literature are measured under static conditions [24,27]. It is known that static and dynamic mechanical properties may very well differ. Nevertheless, the static mechanical properties provide at least an indication of the material properties. Upon application of an external stress, which may be tensile, compressive, or torsional, a solid deforms. Initially, the strain, $\varepsilon$ (dimensionless), increases linearly with stress, $\gamma$ (N/m$^2$):

$$\varepsilon Y = \gamma . \qquad (2)$$

In this region, where Hooke's law applies, it is possible to define Young's modulus, Y (N/m$^2$), as the stress per unit strain. The stress-strain relationship of most tissues can be characterized by three regions [24]. At low stress there is a region of relatively low elastic modulus, in which large extensions may occur for small increases in tension. At high stresses, below the ultimate strength of the tissue, there is a region of high elastic modulus, in which extensions are much smaller for a given stress increment. The slopes in both these regions are approximately linear. In between, at intermediate stresses, there is a region of transition from one linear to the other linear part of the stress-strain curve. No attempt is made here to address these highly complex and, at present, incompletely analyzed problems. The values of the elasticity modulus that were determined for the polyacrylamide gels are clearly measured in the first part of the stress-strain curve. The gels are believed to reach their ultimate strength before the second part of the stress-strain curve is reached. It should be mentioned that the elasticity modulus of compression and tension are typically very similar [27]. However, the ultimate strength due to compression or tension may be very different. In fact, the ultimate strength of the gels has not been determined but is believed to be smaller than that for tissues.

In addition, during holmium laser ablation not only mechanical but also thermal expansion occurs and must be considered as well as the fact that expansion will be three-dimensional rather than one-dimensional. Nevertheless, the static

mechanical properties in the form of the Young's modulus, which is a measure of one-dimensional mechanical deformation, can be used to quantify, in a first-order approximation, the mechanical strength or elasticity of the PAA gels that are used in these experiments.

Overall, the gels are a reasonable representation of biological soft tissues within limitations discussed. The fact that they are transparent and ablation processes can be visualized inside the material outweighs the compromises that have to be made.

### Q-Switched Pulses

The delivery of a Q-switched (500 ns) holmium laser pulse in a highly absorbing medium such as water causes a sequence of events to take place. Initially, the energy is deposited in the material and a subsequent explosion takes place. This initial part is very similar to the well-documented process of underwater explosions due to detonation of an explosive material [16,28]. However, no chemical reaction takes place; the laser energy is deposited at a high rate in the confined volume of irradiated material. The definition of explosion in the context of detonation [16] is a reaction in a substance that converts the original material into a gas at very high pressure and temperature, the process occurring with extreme rapidity and evolving a great deal of heat. The analogy with pulsed infrared laser vaporization easily can be seen, the main difference being that the high pressure and high temperature are due to a vaporization of water by absorbed laser energy.

The first disturbance that is observed within 1 μs after the start of the laser pulse is a pressure wave caused by the heating of the water under stress confinement conditions. This pressure wave, which is often described as a "shock wave," propagates outward, away from the point of origination. Typically this pressure wave has an almost discontinuous rise (the measurement is limited primarily by the detector response time of 40 ns) and a roughly exponential decay. It is assumed that the 1/r scaling law applies to the amplitude of the pressure waves, although there are reports that claim nonlinear effects for high amplitude pressure waves associated with TNT detonation [16] and laser-induced plasma formation [23]. The initial high pressure decreases after the shock wave has been emitted, but it is still much higher than the equilibrium hydrostatic pressure [16]. It has been shown that the amplitude of this thermo-elastic expansion wave is independent of the elasticity modulus of the material, at least within the limits of the materials used.

The absorption coefficients of the water, gel, and tissue at 2.12 μm are comparable ($\mu_a \sim 3$ $mm^{-1}$). Thus for equal radiation conditions, energy depositions in the three materials used in this study should be the same. Consequently, similar pressure buildups are expected, leading to pressure waves that are independent of the materials elasticity. However, it has been reported that for large compressive stress, the stress-strain curve becomes concave upward, which causes the sound speed to increase with stress instead of remaining constant. This causes true shock waves to occur for large stresses [29].

Immediately after the pressure wave moves away from the fiber tip, the first signs of bubble formation are observed after ~1 μs. The water in the immediate vicinity of the forming bubble has a large outward velocity (initially almost 20 m/s) and the diameter of the bubble increases rapidly. It is important to note that in the case of a Q-switched laser pulse, all the energy is delivered before bubble formation starts to take place. The result is that the bubble expands in an almost spherical fashion, only hindered by the physical presence of the fiber and an asymmetric energy deposition (according to Beer's law). The expansion continues for ~100–150 μs, the internal pressure decreases gradually, but the motion persists because of the inertia of the outflowing water [16]. The vapor pressure at later times may actually fall below the equilibrium value. The pressure of the surrounding water brings the outward flow to a stop and the boundary of the bubble starts to contract at an increasing rate. The inward motion continues until the compressibility of the vapor acts as a powerful check to reverse the motion abruptly [16]. This is exactly the time of pressure wave generation. The inertia of the water, together with the elastic properties of the vapor and water, provide the necessary conditions for an oscillating system. The bubble does in fact undergo repeated cycles of expansion and contraction. The number of oscillations is limited by its loss of energy in the form of turbulence and pressure waves. During the contraction phase, water flow is hindered by the delivery fiber. As a consequence, during the last part of the collapse, the bubble is virtually cut in two by the water flow, with one part collapsing at the center of the bubble and one part collapsing at the fiber tip surface. The two collapsing parts each emit a pressure

wave. Sometimes the two pressure waves can be distinguished on the hydrophone trace [13].

A remarkable observation is that although the Q-switched pulse ($\tau_p$ = 500 ns, $H_o$ = 446 mJ/mm$^2$, $Q_o$ = 14 mJ, fiber diameter = 200 μm) has a radiant exposure that is 3.6 times smaller and a pulse energy that is 14.3 times smaller than that of the free running pulses ($\tau_p$ = 100 μs, $H_o$ = 1591 mJ/mm$^2$, $Q_o$ = 200 mJ, fiber diameter = 400 μm), the bubble that is formed is comparable in size (see Figs. 1 and 2). We attribute this to inertia effects, which in the Q-switched pulse where all the energy is deposited in 500 ns are expected to be much larger. This bubble is expected to be "emptier" at its maximum size than the free-running pulses. The bubble induced by the 100 μs, 200 mJ laser pulse is much smaller than would be expected from the energy that is available for vaporization of liquid water [30,31]. We speculate that the relatively smaller bubble induced by the longer pulse durations is caused by heat losses associated with processes like conduction and (forced) convection.

If it is assumed that the water around the bubble is incompressible, it can be shown that the pressure in the bubble depends on the square of the rate of bubble expansion or contraction [16]. From Figure 2, it is evident that this rate is greatest when the bubble is near the point of smallest volume. Therefore, it can be expected from incompressive theory and from the fact that the bubble is under appreciable compression only in this region that pressures will be significant only in a small interval about the time of maximum contraction. This is observed experimentally; pressures waves are emitted that build up to a maximum at the point corresponding to the minimum volume and fall off again as the bubble expands. The lifetime of the bubble (indicated by the moment of collapse) was shown to be linearly dependent on the bubble diameter (Fig. 6). An excellent agreement between our data and the theoretically predicted relation given by Raleigh [15] and Cole [16] was shown:

$$d = 0.0109\ \tau_b \qquad (3)$$

where $d$ is the bubble diameter (in mm), and $\tau_b$ is the bubble life time in μs.

In gels, it is clear that the bubble size will be smaller for gels with a higher elasticity modulus since the elasticity of the gel causes a force that works against bubble expansion. Consequently, the amplitude of the pressure wave at bubble collapse is smaller since the elasticity partially negates the inertia effect and thus the rate of contraction is smaller, leading to a smaller collapse pressure.

In tissue, what happens depends strongly on the particular tissue. It is known from other studies that subsurface bubble formation takes place in aorta [3,32]. When the bubble collapses a pressure wave is induced, whose amplitude and shape depends strongly on the bubble size and bubble geometry. In cartilage, no significant collapse pressure wave has been registered as long as the fiber was in good contact with the tissue. This corresponds to earlier findings in which no significant bubble formation has been associated with ablation of cartilage tissue [32]. Examination of the ablation site, however, did reveal a crater with a diameter that was roughly equal to the fiber diameter. We speculate that meniscus cartilage, which physiological function it is to provide support under compressive stress, may have mechanical properties that are able to deny bubble expansion from taking place. If the fiber and tissue are not in good contact, bubble formation will take place, caused by vaporization of the water between the fiber and tissue. Naturally this will also lead to collapse pressure waves.

### Non-Q-Switched Pulses

In broad lines, the process induced by long pulse durations is similar to the process described for the Q-switched pulses. However, there are a number of significant differences that require explanation.

First, during ablation with the free-running mode pulses (100 μs, 260 μs, 460 μs, and 1,100 μs), the initial thermo-elastic expansion wave is not present. The condition of stress confinement is no longer fulfilled, so pressure that is built up during the initial part of the laser pulse leaves the optical zone by the time the latter parts of the pulse energy are deposited.

Second, bubble onset time increases for increasing pulse durations (Fig. 1). Since the pulse energy is constant, it simply takes more time to deposit sufficient energy to induce vaporization of water by longer pulses. In these cases, the rate of energy deposition is smaller. In addition, other studies have reported an increase in threshold radiant exposure for ablation for increasing pulse durations [30,33]. Although the mechanism behind this is not fully clear, it is generally assumed that it is energy loss due to heat transfer during the laser pulse.

Third, once the bubble starts to form, it grows in length as well as in width. The shorter pulse durations cause a faster rate of growth than the longer pulse durations. It has been observed in this study and in earlier studies that the bubble becomes elongated as the pulse duration increases (Fig. 1) [11,17,34]. Since the latter part of the laser pulse is emitted as the bubble is forming, the laser beam passes through water vapor, which has a small absorption coefficient for the infrared radiation. Thus most of the energy is effectively deposited at the bubble-water boundary, and a channel-like cavity is formed. This phenomena has been described by van Leeuwen et al. [11] as the "Moses effect in the microsecond region." As the pulse duration increases, the first formed parts of the bubble start to collapse while the laser pulse is still causing other parts of the bubble to form and expand. The most extreme example of this is seen in Figure 1e for the 1,100 μs pulse. The results resemble an oscillating system where the top and bottom of the bubble are oscillating out of phase. In addition, the exchange of thermal energy and condensation at the boundary between the vapor inside the bubble and the surrounding water or gel may be different for the shorter pulses as compared to the longer pulses, thus adding to the difference in bubble dynamics due to different pulse durations.

An increase in elasticity modulus of the material in which the laser energy is deposited generally leads to a decrease in bubble size. However, the bubbles induced in the 90% and 95% gel by the 100 μs laser pulse are larger than those in water. No satisfactory explanation for this observation is available at this time. It should be noted that the shapes of the bubble at maximum dimensions are quite different. In water the bubble is almost spherical, whereas in gel the bubble is more elongated. Consequently, although the maximum width and length of the bubble may be larger in these gels, the ultimate bubble volume may be equal or smaller due to the difference in bubble shape. For the 84% water concentration gels, the bubble dimensions were always smaller than in water, regardless of the pulse duration.

Upon collapse of the bubble, a pressure wave is generated. The shape and amplitude of this pressure wave are strongly dependent on the bubble size and its geometry. Therefore, longer pulse durations, which cause more asymmetric bubbles than short pulse durations, cause collapse waves that have smaller amplitudes. The pressure signals associated with asymmetric bubble collapse typically show multiple pressure peaks, relatively close to each other.

In principle, a bubble once formed will collapse regardless of the material in which it is formed. One of the most interesting findings of this study, however, shows that this collapse can be dampened if the laser pulse continues to emit energy while the collapse phase is taking place. It has been observed that the bubble size in water reaches a quasi steady state for pulse durations longer than 460 μs (Figs. 1 and 2). When bubble collapse starts during a laser pulse, there is a significant decrease in contraction velocity and thus in collapse pressure.

### Implications

The implications of this study are potentially significant. It should be kept in mind that pulsed laser ablation of tissue is a tradeoff between unwanted thermal damage caused by long laser pulses (in the extreme cw) and unwanted mechanical damage caused by bubble formation and/or acoustic or pressure waves, induced by short laser pulses [1]. It is generally believed that a significant part of the ablative capabilities of pulsed infrared lasers are due to the explosive vaporization process (i.e., bubble formation). It has been well documented that for the ablation of bone and aorta, tissue is removed by vaporizing water and ejecting tissue fragments [3,35–37]. Therefore, although the process of bubble formation can be minimized, this will be at the expense of the ablative capabilities. It is shown here that the second source of mechanical tissue damage, commonly referred to as acoustic damage, pressure waves, or shock waves, can be significantly reduced while maintaining the ablative capabilities. In addition, there is a legitimate concern about pressure wave damage that may be done to the delivery fiber. By reducing the pressure waves, this risk may also be minimized.

If pressure waves are a concern, Q-switched laser pulses should be avoided. The collapse pressure wave can be minimized by stretching the laser pulse to at least 460 μs, under the experimental conditions described here of a 200 mJ pulse delivered via a 400 μm fiber. This will likely reduce the ablation efficiency for a pulse with a constant energy, but acoustic effects can be reduced by a factor of almost 10. We speculate that for every combination of fiber and pulse energy, a pulse duration can be found that will minimize the pressure wave associated with bubble collapse. Theoretically, this can be done without in-

creasing thermal damage, since the thermal diffusion time is of the order of 100 ms.

In conclusion, bubble geometry and expansion velocity are dependent on the pulse duration. The Q-switched laser pulse is the only pulse duration that meets the conditions of stress confinement and produces a large thermo-elastic expansion wave. During all other pulse durations, pressure waves are generated that are caused by the collapse of the vapor bubble. These pressure waves are dependent on the size and geometry of the vapor bubble. It is concluded that under the given experimental conditions, the acoustic pressure waves can be minimized by stretching the laser pulse. The polyacrylamide gels provide a reasonable model for biological tissue, considering the optical, thermal, and mechanical properties. It has been shown that in gels, which have an elasticity modulus comparable to soft tissue, bubble dimensions and thus collapse pressure waves are smaller than in water.

## ACKNOWLEDGMENTS

The authors thank Brent Bell of the Biomedical Laser and Spectroscopy Program, University of Texas Medical Branch, Galveston, for his assistance with the experiments. We also thank Dr. Klaus Rink of the Laboratory of Applied Optics, Swiss Federal Institute of Technology, Lausanne, Switzerland, for fruitful discussions and his contributions to the manuscript. This research was funded in part by the Office of Naval Research (grant N00014-91-J1564), by the Albert and Clemmie Caster Foundation, by the Swiss optics priority program "Optical Sciences, Applications, and Technologies," and by the NIH (grant 5R01 HL36320 06).

## REFERENCES

1. Welch AJ, Motamedi M, Rastegar S, LeCarpentier GL, Jansen ED. Laser thermal ablation. Photochem Photobiol 1991; 53:815–823.
2. Knopf WD, Parr KL, Moses JW, Cundey PE, Cohen MD, Topaz O, de Marchena E, Lai PY, Kurnik PB, Murphy DR. Multicenter registry report: Holmium laser angioplasty in coronary arteries. Circulation 1992; 86(I) (abstr):511.
3. Van Leeuwen TG, van Erven L, Meertens JH, Motamedi M, Post MJ, Borst C. Origin of arterial wall dissections induced by pulsed excimer and mid-infrared laser ablation in the pig. J Am Coll Cardiol 1992; 19:1610–1618.
4. Könz F, Frenz M, Pratisto H, Weber HP, Lubatschowski H, Kermani O, Ertmer W, Altermatt HJ, Schaffner T. Thermal and mechanical damage of corneal tissue after free running and Q-switched mid-infrared laser ablation. In: van Gemert MJC, Steiner RW, Svaasand LO, Albrecht HJ, Katzir A, eds. "Laser Interaction with Hard and Soft Tissue." Bellingham, WA:SPIE, 1994, pp 78–86.
5. Carome EF, Clark NA, Moeller CE. Generation of acoustic signals in liquids by ruby laser-induced thermal stress transients. Appl Phys Lett 1964; 4:95–97.
6. Bushnell JC, McCloskey DJ. Thermoelastic stress production in solids. J Appl Phys 1968; 39:5541–5546.
7. Jacques SL. Laser-tissue interactions: Photochemical, photothermal and photomechanical. Surg Clin N Am 1992; 72:531–558.
8. Esenaliev RO, Oraevsky AA, Lethokov VS, Karabutov AA, Malinsky TV. Studies of acoustical and shock waves in the pulsed laser ablation of biotissue. Lasers Surg Med 1993; 13:470–484.
9. Dyer PE, Al-Dhahir RK. Transient photoacoustic studies of laser tissue ablation. In: Jacques SL, Katzir A, eds. "Laser-Tissue Interaction I." Bellingham, WA:SPIE, 1990, pp 46–60.
10. Rink K, Delacrétaz G, Salathé RP. Influence of the pulse duration on laser induced mechanical effects. In: MJC van Gemert, RW Steiner, LO Svaasand, H Albrecht, eds. Laser Interaction with Hard and Soft Tissue. Bellingham, WA:SPIE, 1993, pp 181–194.
11. Van Leeuwen TG, van der Veen MJ, Verdaasdonk RM, Borst C. Non-contact tissue ablation by holmium: YSGG laser pulses in blood. Lasers Surg Med 1991; 11:26–34.
12. Asshauer T, Rink K, Delacrétaz G. Acoustic transient generation by holmium laser induced cavitation bubbles. J Appl Phys 1994; 76(9):5007–5013.
13. Frenz M, Pratisto H, Ith M, Asshauer T, Rink K, Delacrétaz G, Romano V, Salathé RP, Weber HP. Transient photoacoustic effects induced in liquids by pulsed erbium lasers. In: Jacques SL, Katzir A, eds. "Laser Tissue Interaction V." Bellingham, WA:SPIE, 1994, pp 402–411.
14. Sedlacek T, Martinelli MA, Esterowitz L, Pinto JF. Reduction of acoustic transients generated in liquid media and in tissue by pulsed 2 μm lasers. In: Jacques SL, Katzir A, eds. "Laser-Tissue Interaction III." Bellingham, WA:SPIE, 1992, pp 302–306.
15. Lord Rayleigh OM, On the pressure developed in a liquid during the collapse of a spherical cavity. Phil Mag S 1917; 34:94–98.
16. Cole RH. "Underwater Explosions." Princeton, NJ: Princeton University Press, 1948.
17. Asshauer T, Rink K, Delacrétaz G, Salathé RP, Gerber B, Frenz M, Pratisto H, Ith M, Romano V, Weber HP. Acoustic transient generation in pulsed holmium laser ablation under water. In: Jacques SL, Katzir A, eds. "Laser-Tissue Interaction V," Bellingham, WA:SPIE, 1994, pp. 423–433.
18. Vogel A, Lauterborn W. Acoustic transient generation by laser-produced cavitation bubbles near solid boundaries. J Acoust Soc Am 1988; 84:719–731.
19. Paltauf G, Reichel E, Schmidt-Kloiber H. Study of different ablation models by use of high-speed sampling photography. In: Jacques SL, Katzir A, eds. "Laser-Tissue Interaction III." Bellingham, WA:SPIE, 1992, pp 343–352.
20. Dingus RS, Scammon RJ. Gruneisen-stress-induced ablation of biological tissue. In: Jacques SL, Katzir A, eds. "Laser-Tissue Interaction II." Bellingham, WA:SPIE, 1991, pp 45–54.

21. Hickling R, Plesset MS. Collapse and rebound of a spherical bubble in water. Phys Fluids 1964; 7:7–14.
22. Schoeffmann J, Schmidt-Kloiber H, Reichel E. Time-resolved investigations of laser-induced shock waves in water by use of polyvinylidenefluoride hydrophones. J Appl Phys 1988; 63:46–51.
23. Doukas AG, Birngruber R, Deutsch TF. Determination of the shock wave pressures generated by laser-induced breakdown in water. In: Jacques SL, Katzir A, eds. "Laser-Tissue Interaction I." Bellingham, WA:SPIE, 1990, pp 61–70.
24. Duck FA. "Physical Properties of Tissue: A Comprehensive Reference Book" London: Academic Press, 1990.
25. Irvine WM, Pollack JB. Infrared optical properties of water and ice spheres. Icarus 1968; 8:324–360.
26. Jansen ED, van Leeuwen TG, Motamedi M, Borst C, Welch AJ. Temperature dependence of the absorption coefficient of water for mid-infrared laser radiation. Lasers Surg Med 1994; 14:259–269.
27. Park JB. "Biomaterials: An Introduction." New York: Plenum Press, 1979.
28. Knapp RT, Daily JW, Hammitt FG. "Cavitation." New York: McGraw-Hill, 1970.
29. Dingus RS, Shafer BP. Laser-induced shock wave effects in materials. In: Jacques SL, Katzir A, eds. "Laser-Tissue Interaction I." Bellingham, WA:SPIE, 1990, pp 36–45.
30. Van Leeuwen TG, Jansen ED, Motamedi M, Borst C, Welch AJ. Excimer laser ablation of soft tissue: a study of the content of fast expanding and collapsing bubbles. IEEE J Quant Elec 1994; 30(5):1339–1345.
31. Jansen ED. Pulsed laser ablation of biological tissue: influence of laser parameters and tissue properties on thermal and mechanical damage, PhD dissertation, University of Texas, Austin, 1994.
32. Jansen ED, Van Leeuwen TG, Verdaasdonk RM, Le TH, Motamedi M, Welch AJ, Borst C. Influence of tissue mechanical strength during UV and IR laser ablation. In: Jacques SL, Katzir A, eds. "Laser-Tissue Interaction IV." Bellingham, WA:SPIE, 1993, pp 139–146.
33. Domankevitz Y, Lee MS, Nishioka NS. Pulsed holmium laser tissue ablation threshold studies. In: Jacques SL, Katzir A, eds. "Laser-Tissue Interaction III." Bellingham, WA:SPIE, 1992, pp 42–45.
34. Loertscher H, Shi WQ, Grundfest WS. Tissue ablation through water with erbium:YAG lasers. IEEE Trans Biomed Eng 1992, 39: 86–87.
35. Izatt JA, Albalgli D, Itzkan I, Feld MS. Pulsed laser ablation of calcified tissue: physical mechanisms and fundamental parameters. In: Jacques SL, Katzir A, eds. "Laser-Tissue Interaction I." Bellingham, WA:SPIE, 1990, pp 133–140.
36. Izatt JA. Pulsed laser ablation of calcified biological tissue: Physical mechanisms and clinical applications, PhD dissertation, MIT, 1991.
37. Walsh JT. Pulsed laser ablation of tissue: Analysis of the removal process and tissue healing, PhD dissertation, MIT, 1988.